EuroIntervention 2019;15:935-938

Dynamic anatomic relationship of coronary arteries to the valves. Part 2: tricuspid annulus and right coronary artery

Ricarda Hinzpeter[1]*, MD; Matthias Eberhard[1], MD; Alberto Pozzoli[2], MD; Robert Manka[1,3,4], MD; Felix C. Tanner[3], MD; Maurizio Taramasso[2], MD; Francesco Maisano[2], MD; Hatem Alkadhi[1], MD, MPH, EBCR, FESER

1. Institute of Diagnostic and Interventional Radiology, University Hospital Zurich, University of Zurich, Zurich, Switzerland; 2. Department of Cardiovascular Surgery, University Hospital of Zurich, University of Zurich, Zurich, Switzerland; 3. Department of Cardiology, University Heart Center Zurich, University of Zurich, Zurich, Switzerland; 4. Institute for Biomedical Engineering, University and ETH Zurich, Zurich, Switzerland

This paper also includes supplementary data published online at: https://eurointervention.pcronline.com/doi/ 10.4244/EIJ-D-19-00670

Introduction

Functional tricuspid regurgitation (FTR) is the most frequent aetiology of tricuspid valve (TV) pathologies and is associated with increased morbidity and mortality[1]. Assessment and management of FTR has developed substantially, in particular because of the increased understanding of the long-term consequences of TV disease together with continued advances in transcatheter techniques[2]. Catheter-based repair requires detailed knowledge of the anatomy of the TV apparatus for planning and periprocedural assistance[3]. Particularly important is the right coronary artery (RCA), which is separated from the tricuspid annulus (TA) by only a few millimetres[4].

This study comprehensively assessed the dynamic anatomic relationship between the TA and RCA in normal subjects and in patients with severe FTR.

Methods

Eighteen patients with severe FTR, determined by transthoracic echocardiography, termed "patients", and 18 patients without cardiac disease, termed "controls", undergoing computed tomography (CT) were included **(Table 1)**. All subjects had right dominant coronary supply.

CT DATA ANALYSIS

Image analysis was carried out using a prototype advanced visualisation, segmentation and image analysis software (3mensio Structural Heart 6.0 beta; Pie Medical Imaging, Maastricht, the Netherlands). TA and RCA dimensions, and distances between the TA and RCA were measured in all phases by two independent readers.

Details regarding CT protocol and statistical analysis can be found in **Supplementary Appendix 1** and **Supplementary Appendix 2**.

Results

DIMENSIONS AND GEOMETRY OF THE TA AND RCA

Patients had a flatter TA and a flatter course of the RCA, coursing in the same plane as the TA, as compared to controls (difference between three-dimensional [3D] and two-dimensional [2D]: maximum lateral diameter in patients: 1.3 mm; in controls 1.5 mm) **(Figure 1)**.

**Corresponding author: Institute of Diagnostic and Interventional Radiology, University Hospital Zurich, Raemistr. 100, CH-8091 Zurich, Switzerland. E-mail: ricarda.hinzpeter@usz.ch*

SUBMITTED ON 19/07/2019 - REVISION RECEIVED ON 30/08/2019 - ACCEPTED ON 10/09/2019

DOI: 10.4244/EIJ-D-19-00670

Table 1. Demographics (mean±SD).

		Patients	Controls	*p*-value
Number of patients		18	18	
Age (years)		68±15	61±12	0.13
Sex	Male	8 (44%)	11 (61%)	0.32
	Female	10 (56%)	7 (39%)	
Body mass index (kg/cm^2)		25±5	27±7	0.27
Left ventricular ejection fraction (%)		56±19	57±14	0.85
Heart rate during CT (bpm)		78±16	74±16	0.49
RCA length (mm)		126.1±12.4	100.1±9.8	<0.001
Annular circumference - systole (mm)		149.8±16	112.9±9	<0.001
Annular circumference - diastole (mm)		155.7±18	116.8±9	<0.001
Annular area - systole (cm^2)		17.8±4	9.8±2	<0.001
Annular area - diastole (cm^2)		19.2±4	10.5±2	<0.001
SD: standard deviation				

TA areas and circumferences were significantly larger and the RCA was significantly longer in patients than in controls in all phases (p<0.001) **(Table 1, Supplementary Table 1)**.

Distances between the TA and RCA were significantly larger in patients than in controls for all measurement points and all phases (p=0.002-0.005) **(Figure 2)**. In controls, the distance between the TA and RCA continuously decreased from proximally to distally throughout phases, while patients had a short segment with increasing distances (seed points 8/9) **(Figure 1, Table 2)**. Both groups showed significantly larger distances proximally than distally (p=0.005-0.01).

The shortest distance between the TA and RCA was found in patients in the distal RCA in end-systole (40%), while in controls the shortest distance was in the distal RCA in end-diastole (90%) **(Table 2)**.

Movement of the RCA in relation to the TA throughout phases, measured between mid-systole (30%) and mid-diastole (70%) showed the largest displacement between the RCA and TA in the mid RCA in controls, while proximal and distal RCA segments showed less movement. Patients showed the largest displacement in proximal and distal segments and less motion in the mid RCA **(Supplementary Figure 1)**.

Discussion

We found consistently longer distances between the TA and RCA in patients compared to controls. Distances between the TA and

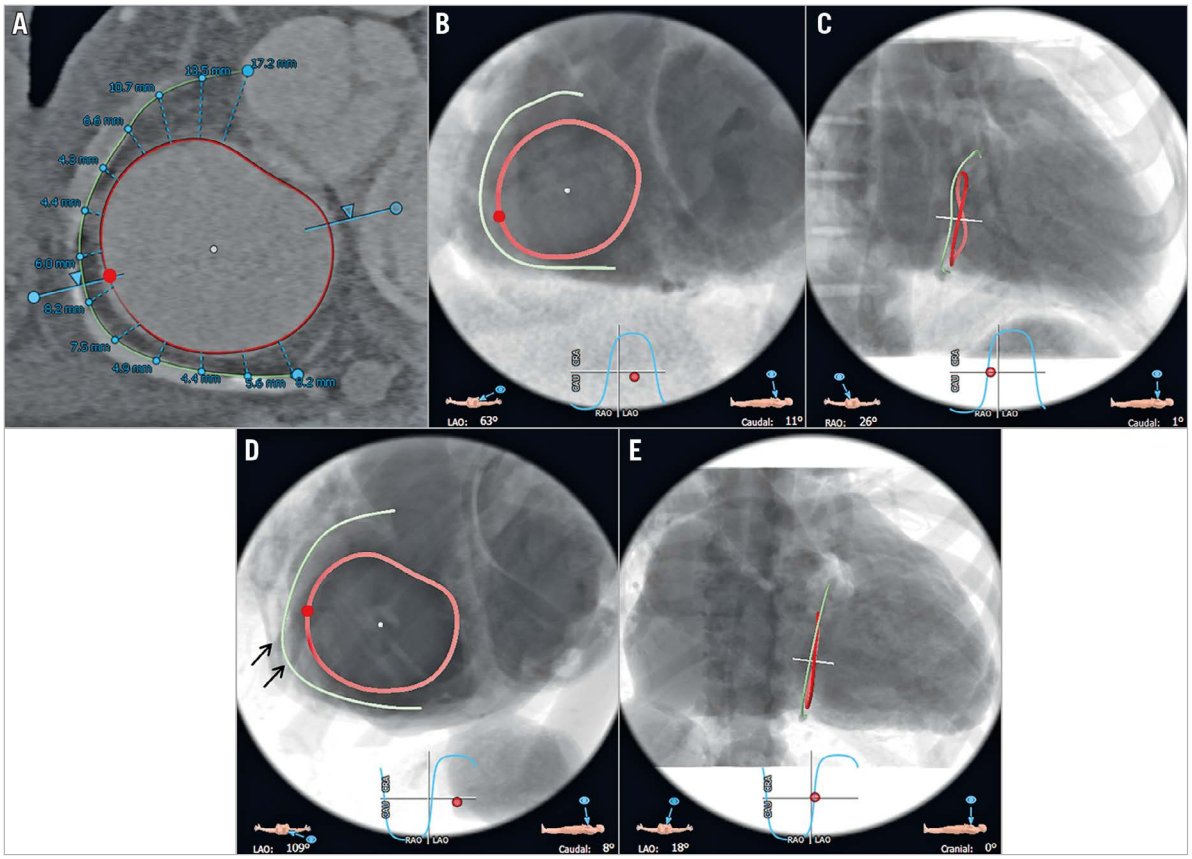

Figure 1. *CT and fluoroscopic views of the TA and RCA in a control and a patient in diastole. CT (A) and fluoroscopic views of the TA and RCA in a control (B: 63° LAO; C: 26° RAO) and a patient (D: 109° LAO; E: 18° LAO) in diastole (80%), including distance measurements of 13 seed points in this representative patient (average number of seed points n=10). Red points: APC (B & D). Black arrows: short segment of the mid RCA in patients with consistent increase in distance to the TA (D), opposite the APC.*

Table 2. Distances between the TA and RCA for all measurements and all phases in both cohorts. Coloured boxes indicate shortest distances. Dark red boxes: shortest overall distances; light red boxes: <7 mm; orange: 7-9 mm; yellow: 9-13 mm; light yellow: >13 mm.

Patients	1	2	3	4	5	6	7	8	9	10	11	12	13	14	15
10%	13.90	13.70	12.50	10.90	9.24	8.45	8.80	9.05	8.64	8.29	7.62	7.70	8.86	8.34	10.28
20%	14.30	14.50	13.39	11.35	9.64	8.49	8.87	9.41	8.69	7.74	6.92	6.94	7.27	6.82	8.75
30%	14.53	15.08	13.78	11.61	9.79	9.13	9.41	9.51	9.15	8.19	7.10	6.77	6.93	7.11	9.06
40%	14.21	14.86	13.65	11.16	9.52	8.83	9.39	9.65	9.26	8.18	7.09	6.64	6.50	6.84	8.45
50%	14.03	14.44	13.02	10.91	9.27	9.30	9.85	9.98	9.17	8.24	7.64	7.51	7.34	7.71	8.05
60%	13.91	13.81	12.50	10.70	9.04	8.38	8.55	8.96	9.14	8.07	7.02	7.72	8.32	7.06	8.18
70%	14.18	13.83	12.40	10.39	8.94	8.83	8.91	8.96	8.68	7.57	7.12	7.30	7.97	7.01	7.15
80%	13.97	13.75	12.69	10.95	9.38	9.04	9.09	8.76	8.14	7.51	6.98	7.16	7.72	6.67	8.13
90%	13.81	13.74	12.74	11.16	9.48	8.82	8.81	8.73	8.08	7.82	7.52	7.83	7.64	7.55	9.25
100%	13.83	13.62	12.30	10.77	9.32	9.04	8.98	8.78	8.90	7.86	7.20	7.64	8.06	7.48	6.80
Controls	**1**	**2**	**3**	**4**	**5**	**6**	**7**	**8**	**9**	**10**	**11**	**12**	**–**	**–**	**–**
10%	13.00	12.80	10.92	8.74	7.91	7.40	7.14	6.50	6.56	6.69	7.60	8.01			
20%	12.43	12.56	11.07	8.56	7.76	7.64	7.21	6.58	6.44	6.19	6.97	7.47			
30%	12.37	12.58	11.49	8.84	8.19	8.00	7.37	7.02	6.21	5.78	6.39	6.58			
40%	12.17	12.47	11.18	8.87	8.42	8.52	7.51	6.80	6.44	5.85	6.56	6.23			
50%	12.99	12.90	11.23	9.33	8.93	8.69	7.70	6.65	5.90	5.42	6.33	5.88			
60%	12.92	13.06	11.56	8.89	8.47	7.93	7.29	6.64	5.79	5.50	6.46	6.47			
70%	13.19	12.92	11.19	8.70	8.21	7.82	6.71	6.05	5.78	5.43	6.16	6.13			
80%	13.07	12.63	11.44	9.19	7.96	7.51	6.89	6.08	5.81	5.95	6.86	7.30			
90%	13.15	12.58	11.32	9.06	7.94	7.48	6.82	6.40	5.78	5.09	6.11	6.33			
100%	13.26	13.27	11.93	9.51	8.65	8.03	7.17	6.53	6.55	6.24	7.35	7.85			

RCA showed a progressive decrease in both groups, being significantly larger proximally than distally, probably due to the larger distances of the proximal/ostial epicardial RCA compared to distal intramuscular segments. Our analyses confirm previous results[4] showing the shortest distances between the posterior TA and distal RCA segment in patients with values between 5.1 and 5.5 mm.

In patients, but not in controls, we consistently found a short segment in the mid-distal RCA, opposite the anteroposterior

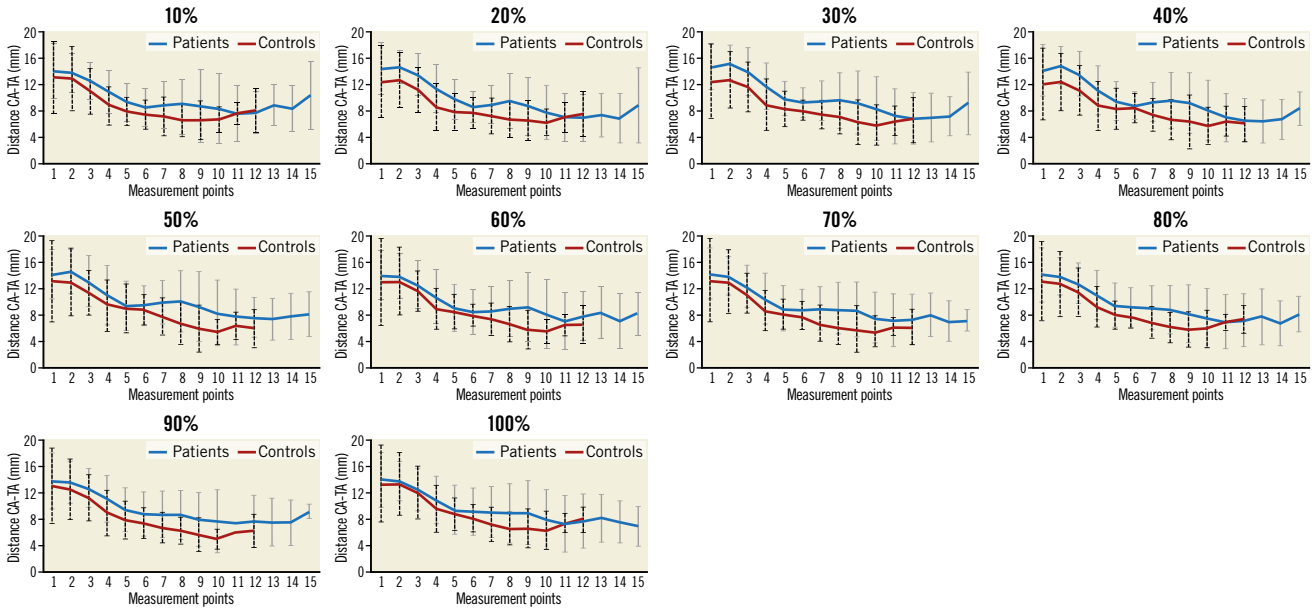

Figure 2. *Distances and SD between the TA and RCA for all measurements and phases in patients (blue line; SD: grey fat line) and controls (red line; SD: black dashed line).*

commissure (APC), showing increasing distance to the TA. This could be explained by differences in the motion patterns of the TA with lower contraction in the anteroseptal to posterolateral direction in patients than in controls, as reported with echocardiography by Fukuda et al[5]. This finding might be relevant as many transcatheter TV replacement techniques target the APC for placing devices.

Limitations

The retrospective design, the small number of patients (none with left coronary dominance), and the study not being performed for a specific device are all limitations.

Conclusion

Our study demonstrates detailed analyses of dynamic 3D motion between the TA and RCA in controls and in patients throughout phases. Distances were larger in controls and continuously decreased from proximally to distally except for a short segment in the mid to distal RCA opposite the APC, where larger distances were found in patients only. This is an important landmark for annuloplasty devices.

Impact on daily practice

Transcatheter therapies for FTR require pre-interventional imaging of the TV geometry and its relationship to surrounding structures such as the RCA to avoid impingement and occlusion of the RCA.

Conflict of interest statement

M. Taramasso is a consultant for St. Jude Medical, and also reports personal fees from Abbott Vascular, Boston Scientific, 4Tech, Edwards Lifesciences and CoreMedic, outside the submitted work. F. Maisano is a co-founder of 4Tech, a consultant for Abbott Vascular, St. Jude Medical, Medtronic and Valtech Cardio, receives royalties from Edwards Lifesciences, and also reports personal fees from Abbott, Edwards Lifesciences, Mitraltech, and other from Edwards Lifesciences, Mitraltech and 4Tech, outside the submitted work. The other authors have no conflicts of interest to declare.

References

1. Hinzpeter R, Eberhard M, Burghard P, Tanner FC, Taramasso M, Manka R, Feuchtner G, Maisano F, Alkadhi H. Computed tomography in patients with tricuspid regurgitation prior to transcatheter valve repair: dynamic analysis of the annulus with an individually tailored contrast media protocol. *EuroIntervention.* 2017;12:e1828-36.

2. van Rosendael PJ, Delgado V, Bax JJ. The tricuspid valve and the right heart: anatomical, pathological and imaging specifications. *EuroIntervention.* 2015; 11:W123-7.

3. Taramasso M, Pozzoli A, Basso C, Thiene G, Denti P, Kuwata S, Nietlispach F, Alfieri O, Hahn RT, Nickenig G, Schofer J, Leon MB, Reisman M, Maisano F. Compare and contrast tricuspid and mitral valve anatomy: interventional perspectives for transcatheter tricuspid valve therapies. *EuroIntervention.* 2018;13:1889-98.

4. Ancona F, Stella S, Taramasso M, Marini C, Latib A, Denti P, Grigioni F, Enriquez-Sarano M, Alfieri O, Colombo A, Maisano F, Agricola E. Multimodality imaging of the tricuspid valve with implication for percutaneous repair approaches. *Heart.* 2017;103:1073-81.

5. Fukuda S, Saracino G, Matsumura Y, Daimon M, Tran H, Greenberg NL, Hozumi T, Yoshikawa J, Thomas JD, Shiota T. Three-dimensional geometry of the tricuspid annulus in healthy subjects and in patients with functional tricuspid regurgitation: a real-time, 3-dimensional echocardiographic study. *Circulation.* 2006;114:I492-8.

Supplementary data

Supplementary Appendix 1. Methods.

Supplementary Appendix 2. Results.

Supplementary Figure 1. Displacement of the RCA in relation to the TA in one cardiac cycle.

Supplementary Table 1. 2D and 3D dimensions of the TA in each phase of the cardiac cycle.

The supplementary data are published online at: https://eurointervention.pcronline.com/doi/10.4244/EIJ-D-19-00670

Supplementary data

Supplementary Appendix 1. Methods

CT data acquisition and image reconstruction

CT examinations were performed on a first- (n=4, SOMATOM Definition; Siemens Healthineers, Forchheim, Germany), second- (n=8, SOMATOM Flash; Siemens) or third-generation dual-source CT scanner (n=6, SOMATOM Force; Siemens). The scan range covered the entire heart in a cranio-caudal direction. All subjects were in sinus rhythm; no β-blockers were given prior to CT.

A standardised triphasic contrast media protocol (Iopromidum, Ultravist 370, 370 mg/ml; Bayer Schering, Berlin, Germany) taking into account the body weight and ejection fraction was used. The total volume of the contrast media was split into 80% at a flow rate of 5 ml/s and 20% at 3.5 ml/s followed by a saline chaser of 30 ml at 3.5 ml/s. Contrast agent application was controlled by bolus tracking in the ascending aorta (attenuation threshold 120 HU at 120 kVp). CT data acquisition was performed with a spiral data acquisition mode synchronised to the electrocardiogram (ECG) in a retrospective mode using ECG pulsing from 30-80% of the RR interval. The average $CTDI_{vol}$ of the protocol was 49±27 mGy. In each patient and control, a total of 10 data sets were reconstructed throughout the cardiac cycle in 10% steps from 0-90% of the RR interval.

CT data analysis

After manually placing 16 seed points along the hinge points of the TA (in the long axis reformation) in each data set, the circumference and the area of the TA were automatically determined as previously described [1]. Subsequently, the RCA was defined by placing seed points along the margin of the vessel facing the TA from the ostium to the origin of the posterior descending artery (PDA). By placing one marker at the ostium of the RCA and one at the origin of the PDA, the length of the vessel was automatically determined. Based on the previously defined TA, shortest distances in the 3D space from the TA to the RCA were generated semi-automatically in 1 cm distances along the RCA (average number of seed points in controls: n=10; average number of seed points in patients with severe FTR: n=11) **(Figure 1)**.

Definition of measurements

In addition to the shortest 3D distances from the TA to the RCA at each seed point, the following measurements of the tricuspid valve apparatus were made:

Area: the annular surface area calculated with projection of the annulus to a plane perpendicular to the mathematical centre of the tricuspid annulus.

Entire TA circumference 3D: the length of the entire annular circumference in 3D.

Entire TA circumference 2D: the length of the entire annular circumference in 3D projected to a 2D plane perpendicular to the mathematical centre.

RCA: the length of the RCA from the right coronary ostium to the origin of the posterior descending artery.

Statistical analysis

Quantitative variables were expressed as means±standard deviations for normally distributed values. Ordinal variables were expressed as frequencies and percentages. Normality was tested using the Shapiro-Wilk test. The χ^2 test was used for differences between groups regarding gender. The Mann-Whitney U test was used for differences between groups regarding age, body mass index (BMI in kg/cm^2), LVEF (in %), heart rate during CT, the length of the RCA and the geometric measurements of the TA. Differences between groups regarding distances of the TA to the RCA were calculated using the Wilcoxon signed-rank test. Differences of distances between the TA and the RCA segments in both groups were calculated using the Wilcoxon signed-rank test. To determine the inter-observer agreement between the two readers, the intraclass correlation coefficient (ICC) was calculated. According to Landis and Koch, ICC values of 0.61-0.80 were interpreted as substantial and 0.81-1.00 as excellent agreement. Additionally, Bland-Altman analysis was performed to assess agreement between the two readers. Data were analysed using commercially available software, SPSS Statistics, Version 25.0 (IBM Corp., Armonk, NY, USA). A two-tailed p-value <0.05 was considered statistically significant.

Supplementary Appendix 2. Results

Interreader agreement

The interreader agreement between readers was high for all measurements of the TA (area in all phases: ICC 0.86-0.99; 2D annular circumference in all phases: ICC 0.84-0.99; 3D annular circumference in all phases: ICC 0.85-0.98) and distances from the TA to the RCA in all phases from all seed points (ICC 0.98-1.0) in both controls and patients with severe FTR. Because of the high interreader agreement, average values from both readers were used for all further analyses. Bland-Altman analyses revealed minimal errors between readers for all measurements in mid-systole (at 30%) and mid-diastole (at 70%) (area: mean difference -0.4±0.8; 95% CI: -1.92-1.19; 2D and 3D annular circumference -1.9±4.5 and -0.6±3.4; 95% CI: -6.91-7.95; distances from the TA to the RCA -0.02±0.9 and -0.4±1.1; 95% CI: -3.12-2.95).

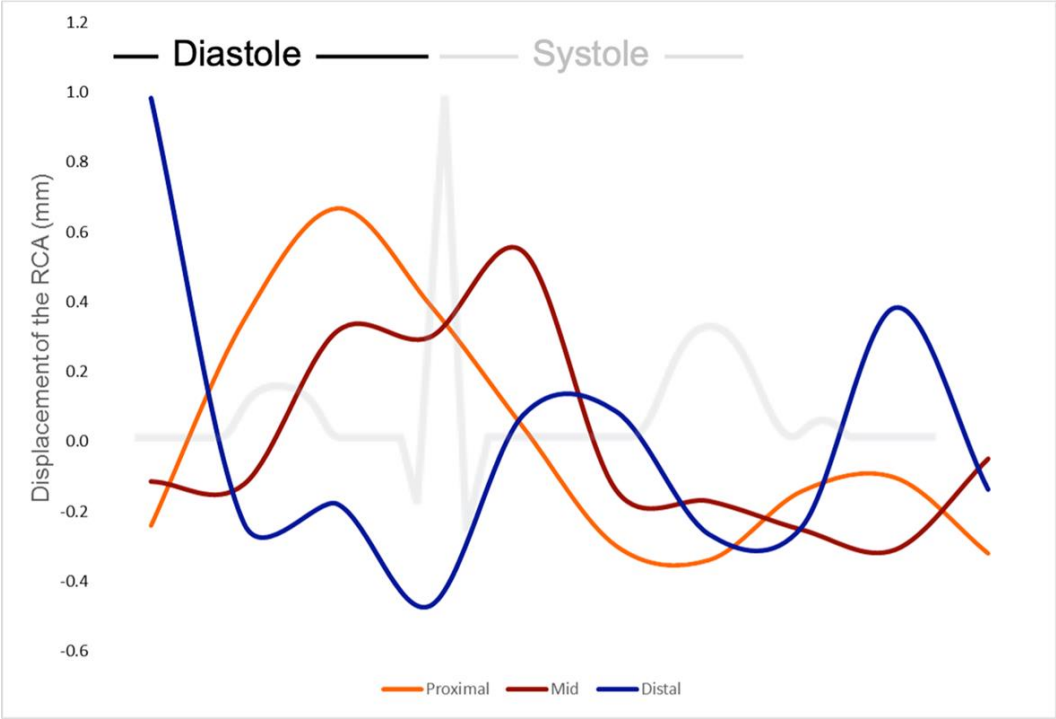

Supplementary Figure 1. Displacement of the RCA in relation to the TA in one cardiac cycle in patients with severe FTR, displayed for the proximal (orange line, mean values of measurement points 1-5), mid (red line, mean values of measurement points 6-10) and distal (blue line, mean values of measurement points 10-15) segments separately. The amplitude indicates the extent of movement between the RCA and TA, with positive values indicating motion of the RCA towards the TA. Note maximum displacement of the RCA in the proximal and mid segments in end-diastole and early systole, respectively.

Supplementary Table 1. 2D and 3D dimensions of the TA in each phase of the cardiac cycle.

	10%	**20%**	**30%**	**40%**	**50%**	**60%**	**70%**	**80%**	**90%**	**100%**
Controls										
Annular area **(cm^2)**	9.5	9.7	9.7	9.6	9.6	10.0	10.2	10.6	10.5	9.5
3D perimeter **(mm)**	113.7	113.3	113.1	113.6	113.7	115.6	116.6	118.9	118.0	112.4
2D perimeter **(mm)**	111.8	112.0	111.4	112.2	112.2	114.4	115.2	117.5	116.5	111.1
Patients with severe FTR										
Annular area **(cm^2)**	19.0	18.7	18.0	18.0	18.1	19.1	19.2	19.5	19.5	19.7
3D perimeter **(mm)**	156.9	154.7	152.2	152.2	153.7	156.3	157.1	158.1	157.6	158.2
2D perimeter **(mm)**	155.0	153.7	150.9	150.6	152.3	155.1	155.9	157	156.7	157.1